Eur. Phys. J. C (2025) 85:179
https://doi.org/10.1140/epjc/s10052-025-13877-9

THE EUROPEAN PHYSICAL JOURNAL C

Regular Article - Theoretical Physics

Accelerated black holes in (2 + 1) dimensions: quasinormal modes and stability

R. D. B. Fontana[1,2,a], **Angel Rincon**[3,b]

[1] Universidade Federal do Rio Grande do Sul, Campus Tramandaí-RS, Estrada Tramandaí-Osório, Tramandaí, RS 95590-000, Brazil
[2] Departamento de Matematica da Universidade de Aveiro and Centre for Research and Development in Mathematics and Applications (CIDMA), Campus de Santiago, 3810-183 Aveiro, Portugal
[3] Departamento de Física Aplicada, Universidad de Alicante, Campus de San Vicente del Raspeig, 03690 Alicante, Spain

Received: 7 November 2024 / Accepted: 26 January 2025

Abstract We investigate the propagation of a scalar field in a (2 + 1)-dimensional accelerated black hole, recently revisited in Arenas-Henriquez et al. (J High Energy Phys https://doi.org/10.1007/jhep05(2022)063, 2022). We briefly describe how the conformal configuration renders a trivial scalar perturbation with a rescaling of the field mass. On the contrary, the free scalar field propagation presents an intricate dynamic, whose equation may be reduced through the use of Israel junction conditions and a non-trivial ansatz. In this case, using two different methods we calculate the quasinormal modes of the solution also obtaining unstable field profiles delivered by the linear scalar perturbation to the background geometry. We examine the parameter space of angular eigenvalues of the field and accelerations under which such instabilities occur.

1 Introduction

Lower dimensional theories of curvature represent an active and important field of research in the present days. Since the pioneering works of Jackiw [2], Mann [3] and Bañados, Teitelboim and Zanelli [4], dating back to the 80 s, a multitude of significant studies were realized, improving the theoretical understanding and broadening the scope of use of their concepts in many directions.

The appealing advantage of such curvature theories is their mathematical simplicity, allowing the study of interesting physical properties as that exhibited e. g. in the AdS/CFT correspondence [5–7]. In many cases, the formalism (even though simpler) strongly resembles that of a four-dimensional gravitational theory, thus representing a theoretical enterprise worth of investigation.

Despite the absence of gravitational freedom, the most straightforward action in (2 + 1) dimensions proposed in [4] (admitting a deep connection with the Chern-Simons theoretical framework [7–9]) presents the interesting solution of an original black hole spacetime: it possesses an event horizon and a conical singularity [10,11].[1] In this geometry, the curvature scalars are smooth but a geodesic incompleteness singularity is found when the spacetime is considered isometric to a globally AdS spacetime. Similar to its higher dimensional counterpart, such solution possesses a fixed (small) number of constants, associated with the black hole physical properties (mass, spin and cosmological constant, and charge investigated a few years later [12,13].

Since the pioneering paper [4], examples of black holes in three dimensions became abundant in the literature. The physical properties of such black holes have been extensively studied (see for instance [14–20] and references therein). Moreover, substantiating the relevance of the topic, textbooks of lower dimensional gravities are now available as, e.g. [2,21] Additionally, different scenarios of those theories were investigated through quantum black holes (or more precisely, solutions with quantum effects) where geometric aspects such as geodesics, the Sagnac effect and thermodynamics, among others are computed (see [22–32] and references therein). It is also worth mentioning the recent summaries of the progress made up to them in the excellent textbook [33].

[a] e-mail: rodrigo.dalbosco@ufrgs.br
[b] e-mail: angel.rincon@ua.es (corresponding author)

[1] It is worth noticing also the solutions of the Jackiw gravity [2] in (1 + 1) dimensions (for a comprehensive survey see [3]) as equally important.

Published online: 13 February 2025

In the present work we will consider a particular case of the Bañados–Teitelboim–Zanelli (BTZ) black hole [4] perturbed to linear order by a probe scalar field. The linear perturbation theory, an important tool for the dynamical analysis of such black holes, was firstly examined in the seminal paper of Regge and Wheeler from 1957 [34]. Since then, a robust development of the field brought the understanding that such black holes perturbations generally evolve as a spectral tower of imaginary frequencies (damped oscillations), the *quasinormal modes* (QNMs).

According to the modern view, perturbations of black holes are described in three different phases: (i) the initial radiation as a response to initial conditions (initial burst), (ii) subsequent damped oscillations characterized by imaginary frequencies (QNMs), and (iii) a power-law decay of the fields. Such complex frequencies characterizing phase (ii) are denoted as $\omega \equiv \omega_R + i\omega_I$ and determined by a few key black hole parameters, namely mass, electric charge and angular momentum [35–39] (see also the seminal monograph [40]). It is noteworthy that the real part of these frequencies governs the oscillation period, expressed as $T = 2\pi/\omega_R$, while the imaginary part is associated with the fluctuation decay with timescale $t_D = 1/\omega_I$.

The existence of such damped modes represents a groundbreaking milestone, measured in the direct observation of gravitational waves by LIGO in black hole mergers [41–43], providing the most compelling evidence to date of the existence of black holes mergers. The discovery has not only confirmed the reality of black holes but has also unveiled an entirely new perspective on our understanding of the universe, trough linear perturbation theory of black hole spacetimes. In such, the quasinormal mode spectra provides unique details about the parameters of the black hole, making possible the determination of its mass and angular momentum.

The study of black hole perturbations and QNMs in 2 + 1 dimensions was performed for the first time for the BTZ solution by Cardoso and Lemos [44] followed by the calculation for the rotating case [5]. More recent papers on the subject can be found in [45–56] and references therein.

Although the expected pattern of evolution of such perturbations is a spectral tower of oscillations (QNMs) followed by the initial burst, under certain circumstances, perturbations delivered by external fields in such systems can destabilize the geometry [47,57–60]. We may see that, in the system we examine in the present work - an accelerated BTZ geometry, that is also the case.

The incorporation of acceleration within a 2 + 1 dimensional spacetime framework is motivated by its potential significance in 3 + 1 general relativity solutions exhibiting non-trivial topology, as originally demonstrated in [61]. This inspiration draws from an analogy with the five-dimensional case, as elaborated in [62].

Accelerating black holes have a plethora of properties distinguishing them from other geometries. First, the spacetime of these black holes come from a conformal line element, known as the C-metric [63–65]. The force driving the acceleration is caused by a conical defect (deficit angle along a polar axis of the black hole): the asymptotic behaviour (experienced by perturbative fields) depends on several parameters of the geometry having a rich dynamics (described in the zoo of C-metric geometries, see e.g. the textbook [66]). Such asymptotic regions can be described by an accelerating horizon, an AdS border or even a cosmological horizon. Studies in which accelerated black holes are examined under different scopes can be found in [67–81] and references therein.

While four-dimensional C-metrics have been extensively studied in their complex aspects [82–89], three-dimensional C-metrics [1,61,90–92], expected to provide a simpler arena for holographic exploration, paradoxically presents a more challenging paradigm [76]. The solution remained almost unexplored until the present being revisited recently [1,91].

Considering the importance of $(2+1)$ gravity as described above, particularly the BTZ black hole and the recent increasing interest in accelerated geometries, in this work we aim to study the scalar field perturbation and corresponding quasinormal modes/instability issues of an accelerated BTZ background.

The paper is structured as follows. Section 2 discusses the main features of the $(2+1)$ accelerated BTZ black hole solution. Then, in Sect. 3, we will introduce the background to be considered in the corresponding scalar perturbations. In the same section, we stablish the basis for computation of the quasinormal modes due to a massless scalar field and discuss the effect of the acceleration on the stability. Our numerical results, as well as some figures and tables, are delivered in Sect. 4, discussing the relative issues brought by the perturbations. Finally, in Sect. 5 we discuss our results and possible perspectives for future work.

2 Background: the (2 + 1) dimensions accelerated BHs

We begin by introducing the accelerated version of the BTZ black hole without rotation and charge as described in [1,61, 90,93] by

$$ds^2 = \Omega^{-2}\Big(- P(y)d\tau^2 + P^{-1}(y)dy^2 + Q^{-1}(x)dx^2\Big), \tag{1}$$

with

$$\begin{aligned} \Omega &= a(x-y), \\ P(y) &= \frac{1}{a^2L^2} + 1 - y^2, \\ Q(x) &= x^2 - 1 \end{aligned} \tag{2}$$

In such geometry, we can insert a strut [1] at a particular $x = x_s$ with induced metric $ds_I^2 = \Omega^{-2}(-Pd\tau^2 + P^{-1}dy^2)$, that allows for the interpretation of a as the acceleration parameter of the geometry. The normal vector to the strut (used to define boundary conditions for motion equations) is written as

$$\mathbf{n} = -\frac{\sqrt{Q_s}}{\Omega}dx. \tag{3}$$

When put into the Israel Junction conditions [94], the geometry presents a negative tension for the strut in the form

$$\mathfrak{T} = -\frac{a}{4\pi}\sqrt{Q_s} \tag{4}$$

with $Q_s = x_s^2 - 1$. In order to find a simple black hole geometry, connected with the original BTZ proposal, we consider another coordinate transformation defined as [1,91]

$$x = \cosh(m\varphi) \tag{5}$$

$$r = -\frac{m}{ay} \tag{6}$$

$$\tau = \frac{t}{ma} \tag{7}$$

in which m represents the constant related to the position of the strut in the geometry established based the above transformation as

$$m = \frac{\text{arccosh}(x_s)}{\pi} \tag{8}$$

The new coordinates bring the metric to a more suitable configuration,

$$ds^2 = \Omega^{-2}\Big(-Fdt^2 + F^{-1}dr^2 + r^2d\varphi^2\Big), \tag{9}$$

with F and Ω given by

$$F = \frac{r^2}{L^2} + m^2(r^2A^2 - 1), \tag{10}$$

$$\Omega = 1 + Ar\cosh(m\varphi). \tag{11}$$

and $a = mA$. Such solution casts a regular accelerated spacetime with an event horizon r_h at $F = 0$, or $r_h = mL(1 - A^2)^{1/2}$ pushed by a strut ($A > 0$). It has a smooth transition to the pure BTZ spacetime whenever $A \to 0$ with m^2 interpreted as the mass of the solution.

With the transformations (5–7), φ represents an angular coordinate mirrored along the x-axis through the strut position: $x = x_s$ whenever $\varphi = \pm\pi$ and $x = x_{min} \equiv 1$ with $\varphi = 0$. In the complete spacetime with the x angular coordinate, the two coordinates patch are defined limited at their boundary by the presence of the strut. For this reason, specific (Israel) boundary conditions have to be considered for the field perturbations as we may further see.

We can obtain other types of spacetimes from the primeval line element (1) by changing the character of the constants and coordinates. Supposing a rotation in the acceleration parameter of type $A \to -A$: the operation reverses the sign of (3) and (4) and – with the proper coordinate adjustments – modify the structure of the spacetime turning its defect into a domain wall. We can also portray the transformation $m \to im$ which brings the solution yet to another accelerated geometry of the BTZ class (viz. a particle without a horizon [92]). In this geometry however, the BTZ solution is not smoothly recovered whenever the acceleration is turned of, and for that reason, we will restrict our analysis to that of an accelerated spacetime with a strut.

We finish this section by quoting relevant papers in the characterization of the accelerated black hole we here study: some thermodynamical aspects of the spacetime were studied in [95], although seminal features as the first law remain an open subject in the literature; semiclassical properties of the scalar field in the spacetime in [96] and the scalar field as part of the background in [93]. Further aspects as the Cotton classification in terms of a null-system can be elucidated through [97,98] and a non-linear version of the charged accelerated black hole can be found in [99].

3 Scalar perturbations

We aim to study the scalar perturbation in an accelerated BTZ black hole through the scattering of a scalar field delivered via matter term,

$$\mathcal{S}_m = -\int_{\mathcal{M}} d^3x\sqrt{-g}\left(\partial_\mu\Phi\partial^\mu\Phi + \varepsilon\Phi^2\right). \tag{12}$$

The motion for such scalar field action is given by

$$\begin{aligned}\Box\Phi - \varepsilon\Phi &= g_{\alpha\beta}\nabla^\alpha\nabla^\beta\Phi - \varepsilon\Phi \\ &= \frac{1}{\sqrt{-g}}\partial_\mu\Big(\sqrt{-g}g^{\mu\nu}\partial_\nu\Phi\Big) - \varepsilon\Phi = 0,\end{aligned} \tag{13}$$

Here we analyze the scalar scattering problem in the geometry (1), in two different scenarios: the free scalar field ($\varepsilon = 0$) and the conformal field with $\varepsilon = \mathcal{R}/8$. The last choice represents a scalar field conformally coupled to the geometry and has the special behavior of a symmetric decouple of the scalar equation relative to the metric without the conformal factor. We explore such situation in the next section with the results (see Eq. (45)).

Following the prescription of [100], we consider a transformation of Φ related to its conformal configuration [101] written as

$$\Phi \to \Omega^{1/2}\psi. \tag{14}$$

With the above relation we start with the free Klein–Gordon equation (we will address the second profile in the next section) casting it into the motion equation as

$$\frac{1}{\sqrt{-\mathfrak{g}}}\partial_\mu\left(\mathfrak{g}^{\mu\nu}\sqrt{-\mathfrak{g}}\partial_\nu\right)\psi+\left(\frac{\mathcal{R}}{8\Omega^2}-\frac{\mathcal{F}}{8}\right)\psi=0, \tag{15}$$

in which $\mathfrak{g}=\text{diag}(-F,F^{-1},r^2)$, and

$$\mathcal{R}=-\frac{6}{L^2} \tag{16}$$

is the Ricci scalar of the geometry and $\mathcal{F}=\mathcal{R}-6m^2A^2$ the Ricci scalar of $\mathfrak{g}$. In order to put equation (15) into a more suitable form, we perform the usual field transformation $\psi\to\zeta/\sqrt{r}$ and implement the tortoise coordinate, $\partial_{r_*}=F\partial_r$ into its derivative operators, obtaining

$$\Omega^2\left(\frac{\partial^2}{\partial r_*^2}-\frac{\partial^2}{\partial t^2}\right)\zeta+\Omega^2F\left(\frac{F}{4r^2}-\frac{\partial_rF}{2r}\right)\zeta$$
$$+\Omega^2F\left(\frac{\partial_{\varphi\varphi}}{r^2}-\frac{\mathcal{F}}{8}\right)\zeta+\frac{\mathcal{R}F}{8}\zeta=0. \tag{17}$$

The above relation (17) reduces to the usual pure BTZ equation [44] when $A=0$ ($\Omega=1$).

For the purpose of integrating (17) we can expand the conformal factor in a vectorial basis $X_k=e^{km\varphi}$,

$$\Omega^2=\sum_{k=-2}^{2}\alpha_kX_k \tag{18}$$

with $\alpha_{-k}\equiv\alpha_k=\left(\frac{Ar}{k}\right)^k$ for $k>0$ and $\alpha_0=1+2\alpha_2$.

Now, in order to match the angular part of (17) with the above, we must take the Klein–Gordon field in a similar basis, with the expansion,

$$\zeta=\Psi\sum_{n_r}\Theta_n, \tag{19}$$

in which Θ_n stands for the angular part of ζ and Ψ the radial-temporal (or double-null) dependence. We write Θ_n in terms of imaginary numbers $n=n_r+in_i$ spanned by the functions X as $\Theta_n=X_{n_r+in_i}$. In the non-accelerated limit we may take $n_r=0$ and recover the usual field decomposition [44].

In order to rewrite Eq. (17) conveniently, we can introduce new operators $\hat{\mathcal{O}}_i$ defined as

$$\hat{\mathcal{O}}_1=\left(\frac{\partial^2}{\partial r_*^2}-\frac{\partial^2}{\partial t^2}\right)+F\left(\frac{F}{4r^2}-\frac{\partial_rF}{2r}-\frac{\mathcal{F}}{8}\right), \tag{20}$$

$$\hat{\mathcal{O}}_2=F\frac{\partial_{\varphi\varphi}}{r^2}, \tag{21}$$

$$\hat{\mathcal{O}}_3=\frac{\mathcal{R}F}{8}, \tag{22}$$

such that Eq. (17) in terms of $\hat{\mathcal{O}}_i$ is pictured as

$$\Omega^2\left(\hat{\mathcal{O}}_1+\hat{\mathcal{O}}_2\right)\zeta+\hat{\mathcal{O}}_3\zeta=0. \tag{23}$$

In the above relation, $\hat{\mathcal{O}}_1$ and $\hat{\mathcal{O}}_2$ act in the angular part of the field allowing Eq. (17) to be separated in the angular basis of vectors X_k.

We analyze the equation for every operator, considering that the sum is not limited (v. g., $mn_r\in\mathbb{Z}$, prescribing a field decomposition). In the end, the equation is rearranged in each pair $\pm n_r$ that respects the angular boundary condition (34). Starting with $\hat{\mathcal{O}}_1$, we have

$$\Omega^2\hat{\mathcal{O}}_1\zeta=\hat{\mathcal{O}}_1\Psi\left(\sum_{k=-2}^{2}\alpha_kX_k\sum_{n_r}X_{n_r}\right)X_{in_i} \tag{24}$$

Since the sum in n_r is taken in every integer value mn_r, each one of the five terms $X_k\sum_{n_r}X_{n_r}$ can be reordered as a simple sum $\sum_{n_r}X_{n_r}$. Then

$$\Omega^2\hat{\mathcal{O}}_1\zeta=(\alpha_0+2\alpha_1+2\alpha_2)\hat{\mathcal{O}}_1\zeta. \tag{25}$$

Similarly, for $\hat{\mathcal{O}}_2$ we can write

$$\Omega^2\hat{\mathcal{O}}_2\zeta=\frac{F}{r^2}\Psi\sum_{k=-2}^{2}\alpha_kX_k\sum_{n_r}n^2m^2X_n \tag{26}$$

and

$$X_{in_i}\sum_{n_r}\sum_{k=-2}^{2}\alpha_kX_k(n_r+in_i)^2m^2X_{n_r}$$
$$=\sum_{n_r}m^2X_n\Big(\alpha_0(n_r+in_i)^2$$
$$+\alpha_1(n_r+in_i-m^{-1})^2+\alpha_{-1}(n_r+in_i+m^{-1})^2$$
$$+\alpha_2(n_r+in_i-2m^{-1})^2+\alpha_{-2}(n_r+in_i+2m^{-1})^2\Big). \tag{27}$$

Since $\alpha_k=\alpha_{-k}$, we can write every term in the rhs of the above equation in terms of a new operator τ to appear in the scalar potential (viz. (32)),

$$\tau=(\tau_++\tau_-)/2,\quad \tau_\pm\equiv\sum_{j=0}^{2}\alpha_jN_j^{(\pm)} \tag{28}$$

in which

$$N_j^{(\pm)}=\frac{2}{(2-j)!}\left(\frac{j^2}{m^2}+(\pm n_r+in_i)^2\right). \tag{29}$$

We still can simplify (28) considering the cancellation of the imaginary term and rewrite

$$\tau=\sum_{j=0}^{2}\alpha_j\frac{2}{(2-j)!}\left(\frac{j^2}{m^2}+n_r^2-n_i^2\right).$$

In such case, the real and imaginary parts of the angular dependence act in opposite direction in the frequencies and the eigenvalue to be considered is the difference between both. Since both n_r and n_i are quantized by the continuity rules, we may rewrite the angular eigenvalue in a different set, $n_r^2 - n_i^2 \equiv \gamma$ emphasizing the difference between both integer numbers, to obtain

$$\tau \equiv \sum_{j=0}^{2} \alpha_j \frac{2}{(2-j)!}\left(\frac{j^2}{m^2} + \gamma\right). \tag{30}$$

We discuss the allowed values for γ in the next subsection.

The last operator, $\hat{\mathcal{O}}_3$ acts trivially on ζ not modifying the angular part of it. After considering all three operators, we summarize the Klein–Gordon equation in the usual form,

$$\left(\frac{\partial^2}{\partial t^2} - \frac{\partial^2}{\partial r_*^2} - \mathcal{V}(r)\right)\Psi = 0, \tag{31}$$

with $\mathcal{V}(r)$ acting as the effective potential,

$$\mathcal{V}(r) \equiv F\left(\frac{\partial_r F}{2r} + \frac{\mathcal{F}}{8} - \frac{F}{4r^2} - \frac{\frac{\mathcal{R}}{8} + \frac{m^2\tau}{r^2}}{\alpha_0 + 2\alpha_1 + 2\alpha_2}\right). \tag{32}$$

We emphasize the need of the two real eigenvalues summed in Eq. (28) seen in the above potential: we can only satisfy the boundary condition (34) once in each equation (31) two modes are concomitantly considered (n_r and $-n_r$).

In the region of integration of the scalar equation, $[r_h, \infty)$, (32) can be entirely positive, partially positive or entirely negative. In Table 1 we analyse the potential according to to three important points: its signal (s_V) in both asymptotic regions and the number of inflections.

The rich structure of $\mathcal{V}(r)$ presented in 1 demonstrates the non-trivial behavior of the propagation of the scalar field in such geometry. By instance, the emergence of an entirely negative potential for a range of accelerations (R_3) is expected to generate unstable profiles (see e. g. [47,57–59,102]). We may see in the next section that, that is not the case here. We represent all the qualitative cases of Table 1 in the Fig. 1.

Despite such rich and oddly shaped potentials, for entirely negative potentials unstable evolutions can not be taken for granted as wee will verify. We assemble the results regarding the dominant frequency and stability analysis in the next section.

3.1 Boundary conditions

The scalar wave equation (31) allows us the investigation of the dynamical aspects of the spacetime considering the field at linear order.

In such equation, the evolution profile can be studied under specific boundary conditions. In the event horizon frontier, we have

$$\left(\frac{\partial^2}{\partial t^2} - \frac{\partial^2}{\partial r_*^2}\right)\Psi \sim 0 \tag{33}$$

bringing the out and inward plane waves $\psi(r) \rightarrow e^{\pm i\omega r_*}$ as possible solutions.[2] In such case, considering the classical scattering problem of relevance – no signal emerges from the horizon, the outgoing wave $e^{+i\omega r_*}$ must be discarded. The field behavior is that of an ingoing frontwave, incident to the event horizon. That is a general condition present in geometries with event horizon and a field motion equation similar to (31), whenever $\mathcal{V}(r)\Big|_{r_h} \rightarrow 0$, as long as no information can emerge from the inner region of the black hole.

In spacetimes with AdS asymptotic structure as the BTZ geometries we are treating, different border terms are possible. In such region, we have,

$$\mathcal{V}(r) = \begin{cases} \mathcal{F}\left(\frac{2+m^2\gamma}{6} - \frac{1}{8A^2L^2}\right) & A \neq 0 \\ \frac{3r^2}{4L^2} & A = 0 \end{cases}$$

which restrains the field character in the frontier. In the second case (non-accelerated) the only meaningful physical boundary term is $\psi(r_\infty) \rightarrow 0$ (Dirichlet). In the first case, we have to choose such term according to the physical problem investigated. In [103] Robin boundary conditions are considered, namely a zero energy flux in the AdS border. In such, the conditions $\partial_r\psi(r_\infty) \rightarrow 0$ (Neumann) and the Dirichlet aforementioned are used with the transition from one to another manipulated with a new variable (maintaining the zero energy flux as the physical constraint).

Other possible set of boundary conditions respecting different wave equations of AdS spacetimes is presented in [104]: plane waves in the AdS infinite modulated by a frequency $\sqrt{\omega^2 - \mathcal{V}_\infty}$, what only applies in cases where $\mathcal{V}_\infty$ is bounded (first case).

In the spacetime we study, the condition of a plane wave in AdS infinite is not physical as long as $\mathcal{V}(r)$ is not smooth in that region when $A \rightarrow 0$. For such reason we consider a particular set inside the Robin boundary conditions [103], that of a zero energy flux in the border with a Dirichlet term. That represents a restraining choice in the possible perturbations in a general class of zero energy flux. It is worth to mention however, that more general boundary terms (Neuman, e. g.) generate oscillations with higher damping, not affecting the fundamental mode.

For the angular part of the field, Θ_n we require that $n_r m \in \mathbf{Z}$ as well as $n_i m \in \mathbf{Z}$, which is also imposed in the pure BTZ geometries ($n_r = 0$). Both assumptions are fundamental to the continuity of Θ_n along the limiting values of the φ axis,

$$\Theta_n(-\pi) = \Theta_n(\pi) \tag{34}$$

with the above chosen Ansatz.

[2] Such condition is accomplished together with the usual decomposition $\psi(t) \rightarrow e^{i\omega t}$.

Table 1 Effective potential behavior with its signal (s_V)for the range of accelerations of the black hole with $r_h = L = 1$ and $\delta = 0$

Region	s_V $(r \to r_h^{(+)})$	s_V $(r \to \infty)$	Number of inflections
R_1 $(A < 0.5)$	$+$	$+$	0
R_2 $(0.5 < A < 0.706)$	$-$	$+$	1
R_3 $(0.706 < A < 0.781)$	$-$	$-$	1
R_4 $(0.781 < A < 0.867)$	$+$	$-$	2
R_5 $(A > 0.867)$	$+$	$+$	1

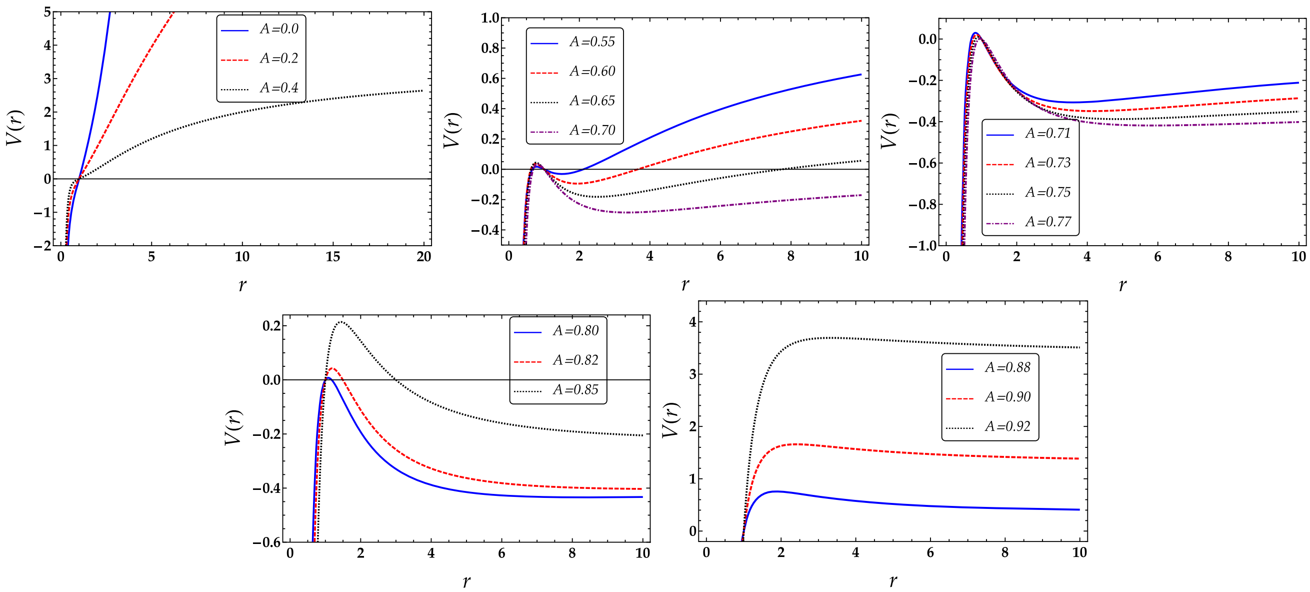

Fig. 1 The scalar field effective potentials for different geometric acceleration ($r_h = L = 1$) with angular momentum $\delta = 0$

In Eq. (30) such condition narrows down the angular eigenvalue γ ($\equiv \delta/m^2$) to another quantization rule,

$$\delta \in \mathbf{Z_s} \tag{35}$$

in which $\mathbf{Z_s}$ is a subgroup of the integer numbers that excludes those multiples of $4\mathbf{Z} + 2$, namely

$$\delta = \pm\{0, 1, 3, 4, 5, 7, 8, 9, 11, 12, 13, \cdots\}. \tag{36}$$

The derivative of the field on the other hand is not continuous in φ (as the metric components are discontinuous as a consequence of the presence of a wall/strut). In such case, the Israel junction conditions [93,94,105] must be considered,

$$n^\mu[\partial_\mu \zeta] = n^\mu \partial_\mu \zeta^+ - n^\mu \partial_\mu \zeta^- = 0, \tag{37}$$

where we recall that n is the normal vector to the strut (3) located at $x = x_s$ and the $\pm$ signals refer to the terminal point of each coordinate patch, $\varphi^\pm = \pm\pi$. We emphasize the limits of φ as mirroring coordinates to the region $\mathbf{R}_x \equiv x \in [1, x_s)$: the negative and positive values of such angular variable render the same image x defined trough (5) in the inteval ($\mathbf{R}_x$) where the spacetime has a physical meaning. In such sense, the above Junction condition must be applied in the terminal points of φ where the strut is located. Yet the field Ansatz (19) can not satisfy the boundary condition (37). However, once we duplicate (19) considering a secondary wave with negative n_i or

$$\zeta = \Psi\Big(X_{in_i} + X_{-in_i}\Big)\sum_{n_r} X_{n_r} = 2\Psi\cos(n_i m\varphi)\sum_{n_r} X_{n_r} \tag{38}$$

equation (37) is fulfilled. Interestingly enough, the wave equation remains unaffected as in (31-32) when we consider the Ansatz (38). The reason is that, summing another equation substituting $n_i \to -n_i$ does not change τ in the potential.

3.2 Numerics

The integration of (31) is performed with an usual technique prescribed firstly in [106] by Gundlach, Price and Pullin. Firstly, we rewrite (31) in double-null coordinates (usually defined, $dv = dr_* + dt$ and $du = dt - dr_*$) obtaining

$$\left(4\frac{\partial^2}{\partial u \partial v} + \mathcal{V}(u, v)\right)\Psi(u, v) = 0. \tag{39}$$

Using such coordinates, we can discretize the wave equation as [107]

$$\Psi_N = \Psi_E + \Psi_W - \Psi_S - \frac{h^2}{8}\mathcal{V}_S\Big(\Psi_W + \Psi_E\Big). \tag{40}$$

Such expression is quite efficient for asymptotically flat or de-Sitter black holes, but its convergence is relatively slow for asymptotically AdS black holes [107]. To circumvent this issue, an alternative integration scheme is

$$\Psi_N = \Big(1 + \frac{h^2}{16}\mathcal{V}_S\Big)^{-1}\Big(\Psi_E + \Psi_W - \Psi_S - \frac{h^2}{16}(\mathcal{V}_S\Psi_S + \mathcal{V}_E\Psi_E + \mathcal{V}_W\Psi_W)\Big), \tag{41}$$

Afterwards we apply in (41) generic Cauchy data,

$$\Psi_{r_* \to 0} = 0, \quad \Psi(u_0, v) = \text{gaussian}(v) \tag{42}$$

that allows for the field evolution and acquisition of the field profile after the above initial burst (42) is imposed. With the signal at hand we finally can apply a spectroscopic technique as the Prony method [107]. It consists of filtering the signal with a specific number of *overtones*, ν

$$\Psi = \sum_{j=1}^{\nu} C_j e^{-i\omega_j t} \tag{43}$$

to which the fundamental is the most expressive, (most influencing in the signal). The filtering is done dividing a particular time interval in the field evolution in a large number of steps and inverting (43) for a specific ν. A thorough description can be found e. g. in [107].

As a double check of our results, we used a secondary method to probe the outcome frequencies of the characteristic integration scheme, the Frobenius expansion as developed by Howoritz and Hubeny [102]. In the Appendix A we elaborate some of the equations needed to perfom the acquisition of the quasinormal frequencies.

4 Results

After the separation of the scalar field equation (39), with a suitable Ansatz (19) and adequate boundary conditions for the angular (34, 37) and radial parts (Dirichlet) we are in position to integrate it and obtain both the field evolution and the quasinormal frequencies. The methods we used were previously described and achieved good convergence in most of the frequencies compared. In what follows we describe the results obtained with the free scalar field wave equation, a rich structure of perturbation with quasinormal modes and instabilities, depending on the acceleration parameter. For completeness, we explore afterward the case of a conformal field, whose results are close to that of a pure BTZ geometry with a rescaling of the cosmological constant.

4.1 Free scalar field

The free scalar field perturbations we studied can be classified into two categories, depending on the field profile evolutions: the stable (quasinormal modes) and the unstable waves. We describe our results in a huge range of geometry/field parameters particularizing for one or another situation.

The fundamental quasinormal modes of the free scalar field (31) can be put into two different sets, depending on the signal of the angular eigenvalue, δ. In both cases, the field perturbations for small $|\delta|$ are stable. Its evolution occurs as a tower of quasimodes after the initial burst. The resultant frequencies of such evolution are shown in Fig. 2 for $|\delta| \leq 1$.

The results displayed in Fig. 2 show interesting peculiarities of the scalar propagation in the accelerated spacetime. First of all the oscillatory nature of the modes is qualitatively unaffected by A, that is, oscillatory waves maintain their behavior ($\omega_r \neq 0$) in the accelerated spacetime, for every value of A, the same being true for purely imaginary evolutions. Second, the existence of positive decoupling constant δ, behavior associated with the presence of the strut in the geometry, diminishes the fundamental frequencies when compared to that found in [44].

The imaginary part of ω behaves qualitatively the same for small $|\delta|$, with increasing acceleration: ω_i achieves a maximum value depending on δ and monotonically decreases from this value on. Such behavior was found in other $(2+1)$D spacetimes, but associated with the change in ω_r (see e. g. [45] and references therein).

An important aspect of the spacetime response to the field perturbation is the oscillation pattern (oscillatory or purely imaginary). In our case such response is defined solely trough the angular constant. When $\delta < 0$ we observe decaying oscillatory profiles dominating the spectrum and whenever $\delta \geq 0$ we have a purely damped profile ($\omega_r = 0$).

In the accelerated BTZ black holes we observe instabilities if $\delta (> 0)$ is sufficiently large. In the pure BTZ limit, frequencies with $\delta > 0$ were never reported as they result from non-usual boundary conditions (not described e. g. in [44]).

The presence of new modes unnoticed in the pure BTZ case whenever $\delta \leq 0$, can be summarized in the limit of very small acceleration ($mA \lesssim 0.01$) with the scale

$$\omega = \frac{\sqrt{-\delta}}{L} - 2\frac{r_h}{L}i, \tag{44}$$

which brings entire new towers of oscillations delimited by (36), not bounded by the condition $\sqrt{-\delta} \in \mathbb{N}$ as in [44]. A table with the oscillatory frequencies for different $\delta < 0$ is provided in Table 2. We notice the numerical results of the first line of Table 2 that perfectly reproduce the scale of (44).

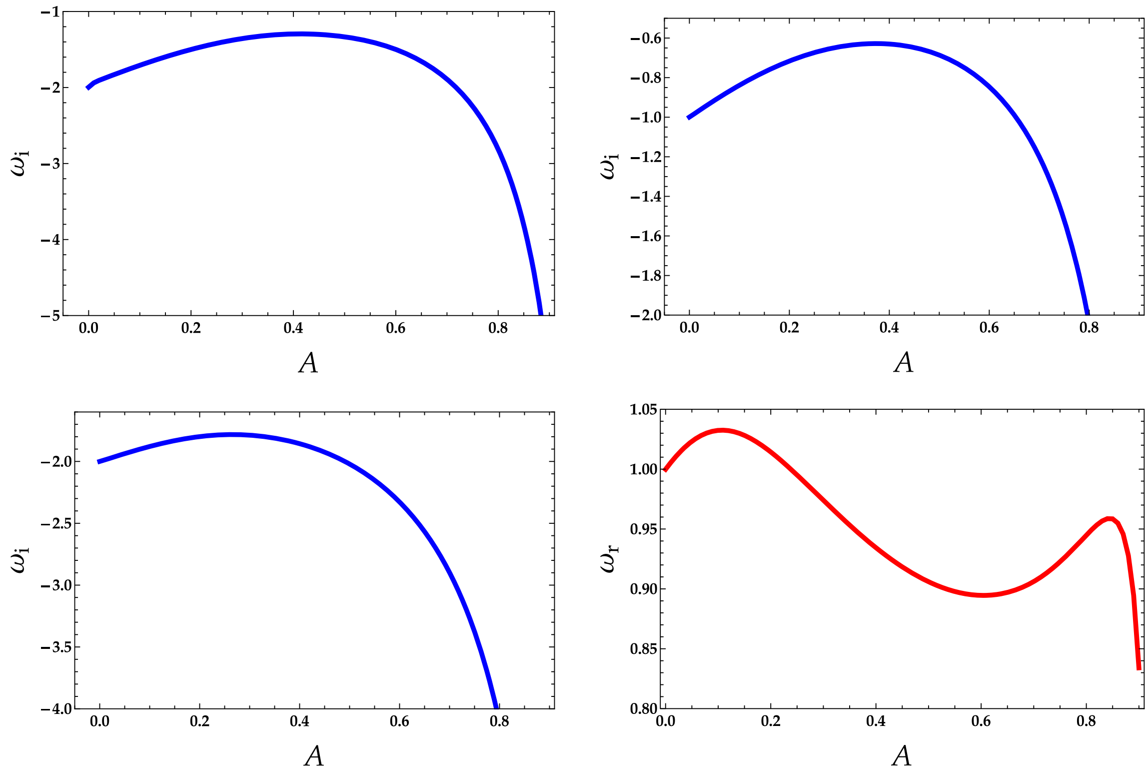

Fig. 2 Quasinormal modes with $\delta = 0$ (top-left panel), $\delta = 1$ (top-right panel) and $\delta = -1$ (bottom panels). The geometry parameters are $r_h = L = 1$

Table 2 Quasinormal modes for negative δ with $r_h = L = 1$.

A	$\delta = -1$	$\delta = -3$	$\delta = -4$	$\delta = -5$
0	0.9999 − 2.000i	1.732 − 2.000i	2.000 − 2.000i	2.236 − 2.000i
0.1	1.032 − 1.879i	1.789 − 1.860i	2.063 − 1.854i	2.304 − 1.849i
0.2	1.014 − 1.799i	1.793 − 1.779i	2.072 − 1.773i	2.317 − 1.768i
0.3	0.9740 − 1.788i	1.789 − 1.777i	2.078 − 1.774i	2.331 − 1.771i
0.4	0.9344 − 1.856i	1.804 − 1.857i	2.109 − 1.857i	2.375 − 1.857i
0.5	0.9060 − 2.021i	1.853 − 2.033i	2.180 − 2.036i	2.464 − 2.038i
0.6	0.8946 − 2.328i	1.952 − 2.350i	2.310 − 2.356i	2.620 − 2.360i
0.7	0.9062 − 2.899i	2.130 − 2.930i	2.535 − 2.938i	2.885 − 2.944i
0.8	0.9449 − 4.109i	2.461 − 4.148i	2.948 − 4.161i	3.367 − 4.170i

Table 3 Quasinormal modes for $\delta \geq 0$ with $r_h = L = 1$

A	$\delta = 0$	$\delta = 1$	$\delta = 3$	$\delta = 4$	$\delta = 5$
0	− 1.996i	− 0.9993i	− 0.2681i	0	0.2358i
0.1	− 1.708i	− 0.8387i	− 0.09255i	0.1807i	0.4212i
0.2	− 1.500i	− 0.7162i	0.02688i	0.3011i	0.5431i
0.3	− 1.356i	− 0.6444i	0.09475i	0.3709i	0.6154i
0.4	− 1.296i	− 0.6302i	0.1140i	0.3957i	0.6458i
0.5	− 1.334i	− 0.6863i	0.07773i	0.3703i	0.6310i
0.6	− 1.500i	− 0.8460i	− 0.04081i	0.2707i	0.5490i
0.7	− 1.890i	− 1.199i	− 0.3193i	0.02423i	0.3319i
0.8	− 2.814i	− 2.038i	− 1.019i	− 0.6172i	− 0.2565i

Table 4 Critical values of acceleration for the scalar instability threshold

δ	A_i	A_s
3	0.18	0.57
4	0	0.70
5	0	0.76

The perturbations with $\delta > 0$ bring the most important issue associated to the scalar field propagation in such spacetime: for $\delta \geq 3$ and a range of values of acceleration, instabilities are present. We list the quasinormal modes and exponential coefficients in Table 3.

In this table, we see oscillations with negative imaginary parts representing quasinormal modes and others with positive coefficient portraying instabilities. The unstable profiles occur in different range of the space of parameters δ and A. Interestingly, for each $\delta > 1$ there is a minimum (A_i) and a maximum (A_s) acceleration that triggers unstable evolution. Examples of such values are summarized in Table 4.

We must emphasize the convergence of the results in Tables 2, 3 and 4 with those obtained in the Frobenius expansion elaborated in the appendix of this work. For $\delta = 0$, the deviation in the fundamental modes does not surpass 0.4% (except in the high acceleration regime) and in most of the other cases (with $\delta \neq 0$) it is limited to 1–2%. The qualitative behavior of the modes is essentially the same as calculated with both methods, with the existence of instabilities being assured in both cases.

The only exception for such good convergence in the frequencies between the results of both methods lies in the transient regions from stable to unstable evolutions, for high δ. Such fact is actually expected as in the threshold regions, the convergence of the Frobenius method is highly affected for the series expansion considered with the nearly stationary configuration, $\omega \sim \omega_R - 0i$ (viz. $\omega_I \sim 0$).

It is worth mentioning however, that the critical values for the accelerations of Table 4 are confirmed in both methods within a deviation of 2%, raising no doubts on the instabilities to linear perturbations on the accelerated spacetime in (2 + 1) dimensions.

The unstable scalar field evolution of linear perturbations in 2 + 1 accelerating black holes is an interesting feature that we stress out to be absent in the 3 + 1 counterparts.

4.2 Conformal scalar configuration

The conformal motion equation (13) of the scalar field in an accelerated BTZ black hole (1) can be extremely simplified with the transformation (14). For such reason we didn't analyze the perturbation in the previous section, since that would be similar to what is reported in [44] (with the addtional coupling term acting as a scalar field mass). If we consider

$$\Box_g \Phi - \frac{\mathcal{R}}{8}\Phi = \Box_{\tilde{g}} \Psi - \frac{\mathcal{F}}{8}\Psi = 0 \tag{45}$$

with the conformal metric $\tilde{g}$ given by $d\tilde{s}^2 = \Omega^2 ds^2$, or $diag(-F, F^{-1}, r^2)$, the system represents the same as the simplest BTZ solution with the cosmological term rescaled as $L^{-2} \to L^{-2} + m^2 A^2$. In this case, we obtain two groups of solutions, the first one possessing the scaling proposed in [5] when Dirichlet boundary conditions are considered,

$$\omega_{(D)} = \pm \frac{n_i}{L} - i \frac{r_h}{L^2}\left(2\nu + 1 + \sqrt{1 + \mu_{eff}^2}\right) \tag{46}$$

in which we emphasize the role played by the term

$$\mu_{eff}^2 \equiv \mathcal{F}/8 = -\frac{3}{4}\left(1 + m^2 L^2 A^2\right) \tag{47}$$

as an effective mass of the scalar field. The second one is that produced by Neumann boundary conditions representing in our case stable solutions [103],

$$\omega_{(N)} = \pm \frac{n_i}{L} - i \frac{r_h}{L^2}\left(2\nu + 1 - \sqrt{1 + \mu_{eff}^2}\right) \tag{48}$$

Interestingly enough, for black holes with $m^2 L^2 A^2 > 1/3$, the mass term acts in the real part of the frequency, breaking the scaling between ω_R and the angular momentum of the field as seen in the pure BTZ solution [44]. We also notice the extra term in the frequencies as the distance of an accelerated version of the BTZ and the non-accelerated spacetime, since $m^2 L^2 A^2 = m^2 L^2 - r_h^2$.

5 Final remarks

In this work, we studied the scalar field perturbation in accelerated (2 + 1) dimensional BTZ geometries. The black hole possesses a topological defect (angular deficit) that results in a strut pushing the spacetime.

Two different field configurations are analyzed, the conformal and the free scalar field, with different outcomes.

The first pattern brings the motion equation to the same as that of the free scalar field in non-accelerated BTZ spacetimes with an effective mass written in terms of the geometric acceleration as in Eq. (47).

The free scalar field representation unleashes a more subtle dynamic. In such regime, we must perform a non-usual field transformation (Ansatz) that leads to a decoupled motion equation (despite the acceleration of the spacetime). The non-trivial boundary conditions are governed by the Israel junction conditions in the patches delimited by the strut.

The decoupled equation was treated with the usual techniques available in the literature (characteristic integration and Frobenius method), with good convergence for the results (quasinormal modes and unstable frequencies) of both methods.

The quasinormal modes ($\delta \leq 0$) maintain the oscillatory pattern considering spacetimes with different accelerations, contrary e. g. to the charged BTZ spacetime [46]. The damping of the field achieves a minimum for intermediate accelerations growing from that point on for increasing A, achieving values considerate high when compared to other BTZ spacetimes.

The results announce an unexpected behavior of the scalar field to linear order, its instability for high enough acceleration or angular eigenvalue. Instabilities triggered by a probe scalar field with non-trivial couplings scenarii [59,60] and/or non-usual global properties are well-represented in the literature from recent [108] to ancient [109] works. To this point it is unclear if the mechanism leading to the particular instability we present in this paper is a liberation mechanism as in the superradiant cases (supporting the evolution of scalar clouds as resolution process to the instability) or an elaborated channel perpetuated at high scale in the entire spacetime that modifies its background as a whole. The answer to such question must be investigated considering a fully non-linear evolution of the perturbations and is outside the scope of our work.

Further lines of investigation include: (i) field perturbations with higher spin and the thermodynamics of scalar field in 2 + 1 dimensional accelerated geometries, or still the quantum-inspired scalar fields on a three-dimensional accelerated geometry.

Acknowledgements A. R. acknowledges financial support from the Generalitat Valenciana through PROMETEO PROJECT CIPROM/2022/13. A. R. is funded by the Universidad de Alicante (María Zambrano contract ZAMBRANO 21-25 (Spain)) (with funding from NextGenerationEU). R. D. B. Fontana thanks the hospitality of DMAT-University of Aveiro/CIDMA and the support of the Center for Research and Development in Mathematics and Applications (CIDMA) through the Portuguese Foundation for Science and Technology (FCT-Fundação para a Ciência e a Tecnologia), references https://doi.org/10.54499/UIDB/04106/2020 and https://doi.org/10.54499/UIDP/04106/2020. The authors also would like to thank to prof. Carlos Herdeiro for insightful suggestions and very fruitful discussions. We are also indebted for enlightening discussions with Dr. Gabriel Arenas-Henriquez for what we are thankful. A. R. acknowledges Gonzalo Olmo for his support and the hospitality of the Departamento de Física Teórica at the Universidad de Valencia, as well as Diego Rubiera García and the hospitality of the Universidad Complutense de Madrid.

Data Availability Statement This manuscript has no associated data. [Author's' comment: This is a theoretical work. No experimental data was used.]

Code Availability Statement Code/software will be made available on reasonable request. [Author's comment: The code/software generated during and/or analysed during the current study is available from the corresponding author on reasonable request.]

Appendix A: Frobenius method

In order to apply the Frobenius method [102] in the wave equation (31) with potential (32), firstly we change the radial coordinate to a more suitable to the boundaries of the spreading problem,

$$u = \frac{r_h}{r} \tag{A1}$$

such that $u_h = 1$ and $u_\infty = 0$. In this system the scalar motion equation turns to

$$\frac{f^2 u^4}{r_h^2}\frac{\partial^2 \Psi}{\partial u^2} + f^2 u \left(\frac{f u}{r_h^2} - \frac{\Delta}{r_h}\right)\frac{\partial \Psi}{\partial u} + (\omega^2 - V)\Psi = 0 \tag{A2}$$

in which $\Delta = (\partial_r F)_x$, $f = F_x$, $V = \mathcal{V}_x$ and x represents the change of coordinate $r \rightarrow u^{-1} r_h$ in each function. The method consists in implementing the expansion

$$\Psi = \sum_{n=0}^{N} (u-1)^{n+\alpha} \tag{A3}$$

in the wave equation, solving the boundary condition near the event horizon implicitly, v. g. choosing the proper α for an ingoing plane wave. To leading order, equation (A2) produces

$$\alpha = \mp \frac{\omega}{\Delta} i. \tag{A4}$$

The upper signal represents an ingoing wave while the bottom accounts for an outgoing that we may ignore.

In a second step, we rewrite equation (A2) performing expansions for each function of the equation as

$$s(u)\frac{\partial^2 \Psi}{\partial u^2} + \tau(u)\frac{\partial \Psi}{\partial u} + \Theta(u)\Psi = 0 \tag{A5}$$

with

$$s(u) = \frac{u^4 f^2}{r_h^2} = \sum_{n=0} s_n (u-1)^n$$

$$\tau(u) = \frac{u^2 f}{r_h^2}(2uf - r_h\Delta) = \sum_{n=0} \tau_n (u-1)^n$$
$$\Theta(u) = \sum_{n=0} \Theta_n (u-1)^n \tag{A6}$$

and

$$\Theta = \omega^2 + m^2\frac{u^2-1}{u^2}\Bigg(-\frac{m^2u^2}{2r_h^2} - \frac{3u^2}{4L^2(u+Ar_h)^2)} + \frac{4\delta u^2 + 8Ar_h u(1+\delta) + 4A^2r_h^2(2+\delta)}{4r_h^2(u+Ar_h)^2}u^2\Bigg) \tag{A7}$$

Finally, solving (A5) order by order, we obtain the recurrence relation for the coefficients a_n,

$$a_n = -\frac{1}{(n^2+2n\alpha)s_2}\sum_{j=0}^{n-1} a_j\Big(\Theta_{n-j} + (\alpha+j)\tau_{n+1-j} + (\alpha^2 + \alpha(2j-1) + j^2 - j)s_{n+2-j}\Big) \tag{A8}$$

The acquisition of the frequencies is done by constructing an algorithm that solves the imaginary polynomial equation derived from the quasinormal condition near infinity, $\Psi_\infty \to 0$, $\Psi(u=0) = 0$ or

$$\sum_{n=0}^{N} a_n(-1)^n = 0 \tag{A9}$$

for a particular N. For such we used the well-known Muller‘s procedure.

References

1. G. Arenas-Henriquez, R. Gregory, A. Scoins, J. High Energy Phys. (2022). https://doi.org/10.1007/jhep05(2022)063
2. R. Jackiw, Nucl. Phys. B **252**, 343 (1985). https://doi.org/10.1016/0550-3213(85)90448-1
3. R.B. Mann, Gen. Relativ. Gravit. **24**, 433 (1992). https://doi.org/10.1007/BF00760418
4. M. Banados, C. Teitelboim, J. Zanelli, Phys. Rev. Lett. **69**, 1849 (1992). https://doi.org/10.1103/PhysRevLett.69.1849. arXiv:hep-th/9204099
5. D. Birmingham, Phys. Rev. D (2001). https://doi.org/10.1103/physrevd.64.064024
6. D. Birmingham, I. Sachs, S.N. Solodukhin, Phys. Rev. Lett. (2002). https://doi.org/10.1103/physrevlett.88.151301
7. E. Witten, (2007). arXiv:0706.3359 [hep-th]
8. E. Witten, Nucl. Phys. B **311**, 46 (1988). https://doi.org/10.1016/0550-3213(88)90143-5
9. A. Achucarro, P.K. Townsend, Phys. Lett. B **180**, 89 (1986). https://doi.org/10.1016/0370-2693(86)90140-1
10. M. Bañados, M. Henneaux, C. Teitelboim, J. Zanelli, Phys. Rev. D **48**, 1506 (1993). https://doi.org/10.1103/PhysRevD.48.1506
11. M. Bañados, M. Henneaux, C. Teitelboim, J. Zanelli, Phys. Rev. D **88**, 069902 (2013). https://doi.org/10.1103/PhysRevD.88.069902
12. S. Carlip, Class. Quantum Gravity **12**, 2853 (1995). https://doi.org/10.1088/0264-9381/12/12/005
13. C. Martínez, C. Teitelboim, J. Zanelli, Phys. Rev. D (2000). https://doi.org/10.1103/physrevd.61.104013
14. D. Birmingham, I. Sachs, S. Sen, Int. J. Mod. Phys. D **10**, 833 (2001). https://doi.org/10.1142/S0218271801001207. arXiv:hep-th/0102155
15. S. Holst, H.-J. Matschull, Class. Quantum Gravity **16**, 3095 (1999). https://doi.org/10.1088/0264-9381/16/10/305. arXiv:gr-qc/9905030
16. D. Birmingham, C. Kennedy, S. Sen, A. Wilkins, Phys. Rev. Lett. **82**, 4164 (1999). https://doi.org/10.1103/PhysRevLett.82.4164. arXiv:hep-th/9812206
17. H.W. Lee, Y.S. Myung, Phys. Rev. D **58**, 104013 (1998). https://doi.org/10.1103/PhysRevD.58.104013. arXiv:hep-th/9804095
18. A. Dasgupta, Phys. Lett. B **445**, 279 (1999). https://doi.org/10.1016/S0370-2693(98)01492-0. arXiv:hep-th/9808086
19. M. Cadoni, M. Melis, Found. Phys. **40**, 638 (2010). https://doi.org/10.1007/s10701-010-9430-6. arXiv:0907.1559 [hep-th]
20. M. Cataldo, N. Cruz, S. del Campo, A. Garcia, Phys. Lett. B **484**, 154 (2000). https://doi.org/10.1016/S0370-2693(00)00609-2. arXiv:hep-th/0008138
21. A.A. García-Díaz, *Exact Solutions in Three-Dimensional Gravity, Cambridge Monographs on Mathematical Physics* (Cambridge University Press, Cambridge, 2017). https://doi.org/10.1017/9781316556566
22. R. Emparan, A.M. Frassino, B. Way, JHEP **11**, 137 (2020). https://doi.org/10.1007/JHEP11(2020)137. arXiv:2007.15999 [hep-th]
23. J. de Oliveira, R.D.B. Fontana, Phys. Rev. D **98**, 044005 (2018). https://doi.org/10.1103/PhysRevD.98.044005. arXiv:1804.00210 [gr-qc]
24. B. Koch, I.A. Reyes, A. Rincón, Class. Quantum Gravity **33**, 225010 (2016). https://doi.org/10.1088/0264-9381/33/22/225010. arXiv:1606.04123 [hep-th]
25. A. Rincón, B. Koch, I. Reyes, J. Phys. Conf. Ser. **831**, 012007 (2017). https://doi.org/10.1088/1742-6596/831/1/012007. arXiv:1701.04531 [hep-th]
26. E. Contreras, A. Rincón, P. Bargueño, Eur. Phys. J. C **79**, 216 (2019). https://doi.org/10.1140/epjc/s10052-019-6749-9. arXiv:1902.02033 [gr-qc]
27. A. Rincón, J.R. Villanueva, Class. Quantum Gravity **37**, 175003 (2020). https://doi.org/10.1088/1361-6382/aba17f. arXiv:1902.03704 [gr-qc]
28. M. Fathi, A. Rincón, J.R. Villanueva, Class. Quantum Gravity **37**, 075004 (2020). https://doi.org/10.1088/1361-6382/ab6f7c. arXiv:1903.09037 [gr-qc]
29. A. Rincón, E. Contreras, F. Tello-Ortiz, P. Bargueño, G. Abellán, Eur. Phys. J. C **80**, 490 (2020). https://doi.org/10.1140/epjc/s10052-020-8071-y. arXiv:2005.10991 [gr-qc]
30. B.E. Panah, K. Jafarzade, Á. Rincón, Gen. Relativ. Gravit. **56**, 46 (2024). https://doi.org/10.1007/s10714-024-03229-5
31. G. Panotopoulos, A. Rincon, Ann. Phys. **443**, 168947 (2022). https://doi.org/10.1016/j.aop.2022.168947. arXiv:2206.03437 [gr-qc]
32. A. Rincon, B. Koch, C. Laporte, F. Canales, N. Cruz, Eur. Phys. J. C **83**, 105 (2023). https://doi.org/10.1140/epjc/s10052-023-11169-8. arXiv:2212.13623 [gr-qc]
33. S. Carlip, *Quantum Gravity in 2 + 1 Dimensions, Cambridge Monographs on Mathematical Physics* (Cambridge University Press, Cambridge, 2003). https://doi.org/10.1017/CBO9780511564192
34. T. Regge, J.A. Wheeler, Phys. Rev. **108**, 1063 (1957). https://doi.org/10.1103/PhysRev.108.1063
35. F.J. Zerilli, Phys. Rev. Lett. **24**, 737 (1970). https://doi.org/10.1103/PhysRevLett.24.737

36. F.J. Zerilli, Phys. Rev. D **2**, 2141 (1970). https://doi.org/10.1103/PhysRevD.2.2141
37. F.J. Zerilli, Phys. Rev. D **9**, 860 (1974). https://doi.org/10.1103/PhysRevD.9.860
38. V. Moncrief, Phys. Rev. D **12**, 1526 (1975). https://doi.org/10.1103/PhysRevD.12.1526
39. S.A. Teukolsky, Phys. Rev. Lett. **29**, 1114 (1972). https://doi.org/10.1103/PhysRevLett.29.1114
40. S. Chandrasekhar, The mathematical theory of black holes (Oxford University Press, Clarendon, Oxford, England and New York, pp. 646, 1983)
41. B.P. Abbott et al. (LIGO Scientific), Virgo. Phys. Rev. Lett. **116**, 061102 (2016). https://doi.org/10.1103/PhysRevLett.116.061102. arXiv:1602.03837 [gr-qc]
42. B.P. Abbott et al. (IGO Scientific, Virgo), Phys. Rev. Lett. **116**, 241103 (2016). https://doi.org/10.1103/PhysRevLett.116.241103. arXiv:1606.04855 [gr-qc]
43. B.P. Abbott et al. (LIGO Scientific, VIRGO), Phys. Rev. Lett. **118**, 221101 (2017). https://doi.org/10.1103/PhysRevLett.118.221101. [Erratum: Phys. Rev. Lett. 121, 129901 (2018)] arXiv:1706.01812 [gr-qc]
44. V. Cardoso, J.P.S. Lemos, Phys. Rev. D (2001). https://doi.org/10.1103/physrevd.63.124015
45. B. Cuadros-Melgar, R.D.B. Fontana, J. de Oliveira, Phys. Rev. D **106**, 124007 (2022). https://doi.org/10.1103/PhysRevD.106.124007. arXiv:2206.06516 [gr-qc]
46. R. Dal Bosco Fontana, (2023). arXiv:2305.05068 [gr-qc]
47. R.D.B. Fontana, (2023). arXiv:2306.02504 [gr-qc]
48. S. Fernando, P.A. González, Y. Vásquez, Eur. Phys. J. C **82**, 600 (2022). https://doi.org/10.1140/epjc/s10052-022-10554-z. arXiv:2204.02755 [gr-qc]
49. A. Ovgün, K. Jusufi, Ann. Phys. **395**, 138 (2018). https://doi.org/10.1016/j.aop.2018.05.013. arXiv:1801.02555 [gr-qc]
50. S. Fernando, Phys. Rev. D **77**, 124005 (2008). https://doi.org/10.1103/PhysRevD.77.124005. arXiv:0802.3321 [hep-th]
51. R. Bécar, P.A. González, E. Papantonopoulos, Y. Vásquez, Eur. Phys. J. C **80**, 600 (2020). https://doi.org/10.1140/epjc/s10052-020-8169-2. arXiv:1906.06654 [gr-qc]
52. A. Anabalón, O. Fierro, J. Figueroa, J. Oliva, Eur. Phys. J. C **79**, 281 (2019). https://doi.org/10.1140/epjc/s10052-019-6748-x. arXiv:1901.00448 [hep-th]
53. P.A. González, A. Rincón, J. Saavedra, Y. Vásquez, Phys. Rev. D **104**, 084047 (2021). https://doi.org/10.1103/PhysRevD.104.084047. arXiv:2107.08611 [gr-qc]
54. A. Rincón, G. Panotopoulos, Eur. Phys. J. C **78**, 858 (2018). https://doi.org/10.1140/epjc/s10052-018-6352-5. arXiv:1810.08822 [gr-qc]
55. A. Rincón, G. Panotopoulos, Phys. Rev. D **97**, 024027 (2018). https://doi.org/10.1103/PhysRevD.97.024027. arXiv:1801.03248 [hep-th]
56. G. Panotopoulos, A. Rincón, Phys. Lett. B **772**, 523 (2017). https://doi.org/10.1016/j.physletb.2017.07.014. arXiv:1611.06233 [hep-th]
57. Z. Zhu, S.-J. Zhang, C. Pellicer, B. Wang, E. Abdalla, Phys. Rev. D (2014). https://doi.org/10.1103/physrevd.90.044042
58. R. Konoplya, A. Zhidenko, Phys. Rev. D (2014). https://doi.org/10.1103/physrevd.90.064048
59. R.D.B. Fontana, J. de Oliveira, A.B. Pavan, Eur. Phys. J. C (2019). https://doi.org/10.1140/epjc/s10052-019-6831-3
60. E. Abdalla, B. Cuadros-Melgar, R. Fontana, J. de Oliveira, E. Papantonopoulos, A. Pavan, Phys. Rev. D (2019). https://doi.org/10.1103/physrevd.99.104065
61. M. Astorino, J. High Energy Phys. (2011). https://doi.org/10.1007/jhep01(2011)114
62. R. Emparan, H.S. Reall, Living Rev. Relativ. **11**, 6 (2008). https://doi.org/10.12942/lrr-2008-6. arXiv:0801.3471 [hep-th]
63. W. Kinnersley, M. Walker, Phys. Rev. D **2**, 1359 (1970). https://doi.org/10.1103/PhysRevD.2.1359
64. J.F. Plebanski, M. Demianski, Ann. Phys. **98**, 98 (1976). https://doi.org/10.1016/0003-4916(76)90240-2
65. J.B. Griffiths, J. Podolsky, Int. J. Mod. Phys. D **15**, 335 (2006). https://doi.org/10.1142/S0218271806007742. arXiv:gr-qc/0511091
66. J.B. Griffiths, J. Podolsky, *Exact Space-Times in Einstein's General Relativity, Cambridge Monographs on Mathematical Physics* (Cambridge University Press, Cambridge, 2009). https://doi.org/10.1017/CBO9780511635397
67. M. Appels, R. Gregory, D. Kubiznak, Phys. Rev. Lett. **117**, 131303 (2016). https://doi.org/10.1103/PhysRevLett.117.131303. arXiv:1604.08812 [hep-th]
68. M. Astorino, Phys. Rev. D **95**, 064007 (2017). https://doi.org/10.1103/PhysRevD.95.064007. arXiv:1612.04387 [gr-qc]
69. A. Anabalón, M. Appels, R. Gregory, D. Kubizňák, R.B. Mann, A. Ovgün, Phys. Rev. D **98**, 104038 (2018). https://doi.org/10.1103/PhysRevD.98.104038. arXiv:1805.02687 [hep-th]
70. R. Gregory, A. Scoins, Phys. Lett. B **796**, 191 (2019). https://doi.org/10.1016/j.physletb.2019.06.071. arXiv:1904.09660 [hep-th]
71. J. Zhang, Y. Li, H. Yu, JHEP **02**, 144 (2019). https://doi.org/10.1007/JHEP02(2019)144. arXiv:1808.10299 [hep-th]
72. K. Destounis, R.D.B. Fontana, F.C. Mena, Phys. Rev. D **102**, 044005 (2020). https://doi.org/10.1103/PhysRevD.102.044005. arXiv:2005.03028 [gr-qc]
73. A. Ball, Class. Quantum Gravity **38**, 195024 (2021). https://doi.org/10.1088/1361-6382/ac2139. arXiv:2103.07521 [hep-th]
74. M. Zhang, J. Jiang, Phys. Rev. D **103**, 025005 (2021). https://doi.org/10.1103/PhysRevD.103.025005. arXiv:2010.12194 [gr-qc]
75. B. Eslam Panah, K. Jafarzade, Gen. Relativ. Gravit. **54**, 19 (2022). https://doi.org/10.1007/s10714-022-02904-9. arXiv:1906.09478 [hep-th]
76. B. Eslam Panah, M. Khorasani, J. Sedaghat, Eur. Phys. J. Plus **138**, 728 (2023). https://doi.org/10.1140/epjp/s13360-023-04339-w. arXiv:2309.02472 [gr-qc]
77. B. Eslam Panah, Phys. Lett. B **844**, 138111 (2023). https://doi.org/10.1016/j.physletb.2023.138111
78. M. Nozawa, T. Kobayashi, Phys. Rev. D **78**, 064006 (2008). https://doi.org/10.1103/PhysRevD.78.064006
79. D. Klemm, M. Nozawa, J. High Energy Phys. **2013**, 123 (2013). https://doi.org/10.1007/JHEP05(2013)123
80. M. Nozawa, T. Torii, Phys. Rev. D **107**, 064064 (2023). https://doi.org/10.1103/PhysRevD.107.064064
81. M. Nozawa, T. Torii, Phys. Rev. D **108**, 064036 (2023). https://doi.org/10.1103/PhysRevD.108.064036
82. P.S. Letelier, S.R. Oliveira, Phys. Rev. D **64**, 064005 (2001). https://doi.org/10.1103/PhysRevD.64.064005. arXiv:gr-qc/9809089
83. J. Bicak, V. Pravda, Phys. Rev. D **60**, 044004 (1999). https://doi.org/10.1103/PhysRevD.60.044004. arXiv:gr-qc/9902075
84. J. Podolsky, J.B. Griffiths, Gen. Relativ. Gravit. **33**, 59 (2001). https://doi.org/10.1023/A:1002023918883. arXiv:gr-qc/0006093
85. V. Pravda, A. Pravdova, Class. Quantum Gravity **18**, 1205 (2001). https://doi.org/10.1088/0264-9381/18/7/305. arXiv:gr-qc/0010051
86. O.J.C. Dias, J.P.S. Lemos, Phys. Rev. D **67**, 064001 (2003). https://doi.org/10.1103/PhysRevD.67.064001. arXiv:hep-th/0210065
87. J. Barrientos, A. Cisterna, D. Kubizňák, J. Oliva, Phys. Lett. B **834**, 137447 (2022). https://doi.org/10.1016/j.physletb.2022.137447
88. J. Barrientos, A. Cisterna, Phys. Rev. D (2023). https://doi.org/10.1103/physrevd.108.024059
89. J. Barrientos, A. Cisterna, K. Pallikaris, Gen. Relativ. Gravit. (2024). https://doi.org/10.1007/s10714-024-03304-x

90. W. Xu, K. Meng, L. Zhao, Class. Quantum Gravity **29**, 155005 (2012). https://doi.org/10.1088/0264-9381/29/15/155005
91. G. Arenas-Henriquez, A. Cisterna, F. Diaz, R. Gregory, Accelerating black holes in $2 + 1$ dimensions: holography revisited. (2023). arXiv:2308.00613 [hep-th]
92. G. Arenas-Henriquez, Many phases of accelerating black holes in 2+1 dimensions, Ph.D. thesis, Durham University (2023)
93. A. Cisterna, F. Diaz, R.B. Mann, J. Oliva, J. High Energy Phys. (2023). https://doi.org/10.1007/jhep11(2023)073
94. W. Israel, Nuovo Cimento B Serie **44**, 1 (1966). https://doi.org/10.1007/BF02710419
95. J. Tian, T. Lai, Thermodynamics and holography of three-dimensional accelerating black holes. (2024). arXiv:2312.13718 [hep-th]
96. M.M. Anber, J. High Energy Phys. **2008**, 026–026 (2008). https://doi.org/10.1088/1126-6708/2008/11/026
97. J. Podolsky, M. Papajcik, A novel classification method of 2+1 spacetimes based on the cotton scalars. (2023). arXiv:2310.10528 [gr-qc]
98. M. Papajcik, J. Podolsky, Algebraic classification of 2+1 geometries: a new approach. (2023). arXiv:2311.00872 [gr-qc]
99. B. Eslam Panah, Fortschritte der Physik (2023). https://doi.org/10.1002/prop.202300012
100. R.M. Wald, *General Relativity, University of Chicago Press* (University of Chicago Press, Chicago, 1984). https://doi.org/10.7208/chicago/9780226870373.001.0001
101. R.D. Fontana, F.C. Mena, J. High Energy Phys. (2022). https://doi.org/10.1007/jhep10(2022)047
102. G.T. Horowitz, V.E. Hubeny, Phys. Rev. D (2000). https://doi.org/10.1103/physrevd.62.024027
103. C. Dappiaggi, H.R. Ferreira, C.A. Herdeiro, Phys. Lett. B **778**, 146 (2018). https://doi.org/10.1016/j.physletb.2018.01.018
104. C.-H. Chen, H.-T. Cho, A.S. Cornell, Chin. J. Phys. **67**, 646–656 (2020). https://doi.org/10.1016/j.cjph.2020.08.015
105. E. Poisson, *A Relativist's Toolkit: The Mathematics of Black-Hole Mechanics* (Cambridge University Press, Cambridge, 2004)
106. C. Gundlach, R.H. Price, J. Pullin, Phys. Rev. D **49**, 883 (1994). https://doi.org/10.1103/physrevd.49.883
107. R. Konoplya, A. Zhidenko, Rev. Mod. Phys. **83**, 793 (2011). https://doi.org/10.1103/RevModPhys.83.793. arXiv:1102.4014 [gr-qc]
108. V. Cardoso, S. Mukohyama, N. Oshita, K. Takahashi, Black holes, multiple propagation speeds and energy extraction. (2024). arXiv:2404.05790 [gr-qc]
109. R. Gregory, R. Laflamme, Phys. Rev. Lett. **70**, 2837–2840 (1993). https://doi.org/10.1103/physrevlett.70.2837